2-7 Calibration of SAR Probe

Lira HAMADA and Soichi WATANABE

The calibration of a specific absorption rate probe is namely a calibration of the electric field measurement sensor in the phantom liquid of high electric loss. The standard electric field method that uses the rectangular waveguide filled with phantom liquid is widely used for the probe calibration. NICT is only institute to serve the calibration for the probe. In this text, the calibration procedure of this waveguide calibration technique is described, along with the detailed procedure, the calibration result, and the uncertainty evaluation. Moreover, this text introduces other calibration techniques.

1 Introduction

Specific Absorption Rate (SAR) is one index for assessing electromagnetic field exposure from devices and equipment that emit electromagnetic waves such as mobile wireless devices and base stations. In Japan and overseas, SAR limitation values are established based on radio-radiation protection guidelines [1]–[6], and are mainly applied to wireless communication devices used near the human body, such as mobile phones. Therefore, for wireless communication devices such as mobile phones, compliance evaluation to radio-radiation guidelines are legislated under the standards and regulations in Japan and overseas [7]–[10].

Measurement equipment used in tests of wireless communication devices must be calibrated periodically, based on regulations. In tests to assess compliance with SAR limit, a SAR probe is used to measure SAR, and the SAR probe must be calibrated. NICT is the only institution performing SAR probe calibration service in Japan.

This paper describes SAR probe calibration at NICT. Several SAR probe calibration methods have been standardized in Japan and overseas. Explained here are the principles of three major methods, including detailed steps and examples for measurement and uncertainty evaluation for the waveguide calibration method used in the calibration work of NICT.

2 Definitions [7]

2.1 Radio-radiation protection guideline [1]

Recommended guidelines for safe conditions under which the exposure level of electromagnetic waves is considered not to cause possible undesirable biological effects on the human body (considering the frequency range from 10 kHz to 300 GHz).

2.2 Specific Absorption Rate (SAR) [1]

SAR is electric power absorbed by biological tissues (lossy dielectric). SAR in lossy media (such as phantom liquid) is related to both the electric field (E) and the gradient of changes over time of temperature (dT/dt) in media. Therefore, the equation below is provided based on this relationship.

$$SAR = \sigma \frac{E^2}{\rho} = c_k \frac{dT}{dt}\Big|_{t=0} \quad (1)$$

Here, the variables are:

σ Conductivity
ρ Density of the media
C_k Specific heat

From Equation (1), an electric field in lossy media can be measured indirectly by measuring the temperature gradient in that media. A temperature probe that has fast response time (less than 1 second) at high spatial resolution but does not disturb the electromagnetic field (optical fiber probe or a thermistor probe using a resistance wire) can be used.

2.3 Local exposure guideline [1]

The guideline is used for electromagnetic fields that have a partial absorption on part of the human body, caused by electromagnetic waves emitted from, for example, wireless devices used very close to the human body.

2.4 Local SAR [1]

SAR is provided as a value per very small volume. It distributes spatially dependent on the location in the biotissues and exposure conditions of the electromagnetic waves. For this distribution, SAR averaged over the localized volume containing a certain mass of tissue such as 1 g or 10 g is called local SAR; the maximum value is called local peak SAR. However, in assessing compliance with guidelines to protect electromagnetic field exposure in Japan, the average volume is defined as a 10 g cube of tissue, and assessed as a time -average during 6 arbitrary minutes.

2.5 Phantom [1]

This is a quasi-human model used to estimate SAR experimentally. If the uniform material is used across the entire model, then it is called a uniform phantom. If it models the electrical characteristics for each corresponding tissue, then it is called an inhomogeneous phantom. SAR measurements use a uniform phantom comprised of an outer shell (container) to model the human body shape, and the liquid (phantom liquid) is filled inside the shell.

Table 1 Dielectric constants of phantom liquid: Example of standard values

Frequency (MHz)	ε_r'	Conductivity σ (S/m)
733	*41.9*	*0.89*
835	41.5	0.90
1450	40.5	1.20
1624	*40.3*	*1.30*
1767.5	*40.0*	*1.38*
1950	40.0	1.40
2018	*40.0*	*1.42*
2450	39.2	1.80
2585	*39.0*	*1.94*
3500	38.5	2.40
5200	*36.0*	*4.66*

Numbers in italics are obtained by interpolation between frequencies

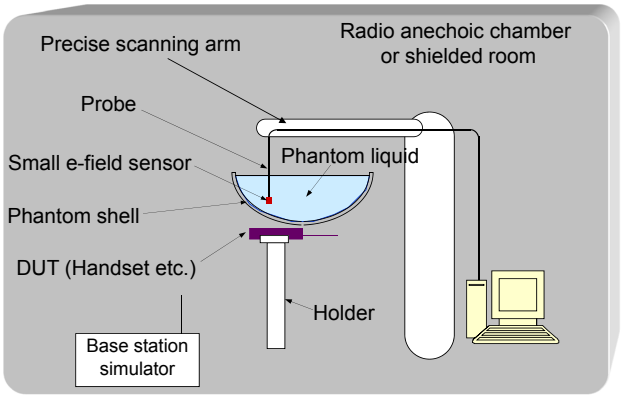

Fig. 1 Diagram of SAR measurement equipment

Therefore, SAR probe calibration also requires determination of the calibration factor in phantom liquid.

2.6 Phantom liquid [1]

Electrical characteristics of phantom liquid filled in the phantom are in accordance with standard values of frequencies of SAR measurement methods such as in IEC 62209–1 [8], which establishes standard values at several frequencies in 30 MHz – 6 GHz. Values of frequencies not in the standard are given by linear interpolation. Table 1 shows dielectric constants at calibration frequencies of NICT.

2.7 Boundary effect [11]

Change of the sensitivity of electric probe caused by the existing boundary between different dielectric medium. When, for example, the probe tip is near the dielectric container surface, this effect appears as the probe sensitivity change.

3 Structure and calibration factor of SAR measurement probe [12][13]

First, Fig. 1 shows an actual SAR measurement system for wireless devices, and Fig. 2 shows a typical probe structure. A SAR probe is an electric field measurement sensor used in lossy phantom liquid. Therefore, the calibration factor (or sensitivity coefficient) is the value that relates the incident electric field and output voltage of the SAR probe; this is not different from ordinary antenna calibration in free space. However, as the calibration factor of the SAR probe is affected by the dielectric constant of surrounding media, the calibration factor in the phantom liquid has to be determined in SAR measurements. The details of the SAR measurement methods are left for Chapter **3-3**, and please refer to the chapter to see how the SAR probe is used in the measurement.

A typical SAR probe structure has sensors comprised of a Schottky diode inserted between elements of three tiny dipole antennas (i = 0 to 2), arranged in a triangular structure for a 3-axis orthogonal antenna [11]. The output voltage V_i of the SAR probe in proportion to the square of the electric field strength E_i in the position of each sensor due to the squared detection characteristics of the diodes. The electric field strength E in centers of the sensor is given by the sum of the squares of the electric field strength that these three sensors receive. Here, K_i is the calibration factor of each sensor.

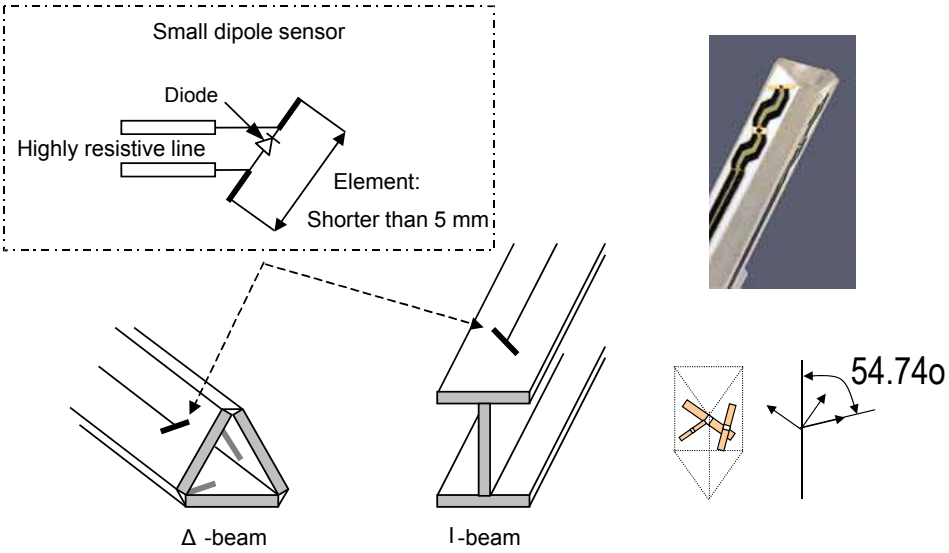

Fig. 2 Structure of SAR probe

$$|E|^2 = \sum_{i=0}^{2} |E_i|^2 = \sum_{i=0}^{2} \frac{V_i}{K_i} \tag{2}$$

The voltage U_i actually detected in each sensor is affected by the non-linearity of diode compression DCP_i. Thus, as an example, correction (calibration of DCP_i) by Equation (3) is performed as per below and converted into the voltage V_i assumed in Equation (2).

$$V_i = U_i + \frac{U_i^{\,2}}{1000 \times DCP_i} \tag{3}$$

Also, the calibration factor K_i can be expressed as the sensitivity coefficient NF_i of each sensor in free space, multiplied by the conversion factor which is the ratio of the sensitivity coefficient in free space to that in phantom liquid.

$$K_i = NF_i \times Factor \tag{4}$$

The conversion factor is assumed to not depend on each sensor. Thus, by taking the detection voltage U_i of the SAR probe at the calibration position and applying it into Equation (5) below, the *Factor* can be calculated.

$$Factor = |E|^{-2} \sum_{i=0}^{2} NF_i^{-1} \left(U_i + \frac{U_i^{\,2}}{1000 \times DCP_i} \right) \tag{5}$$

If the SAR probe has three sensors as shown in Fig. 2, these steps can be performed: first the sensitivity coefficient NF_i in free space of the three sensors in a rectangular waveguide or at the TEM cell is obtained, then the sensitivity coefficient in phantom liquid is obtained, and then finally the calibration factor K_i is determined. NICT provides K_i as the calibration factor.

4 Principles of probe calibration

Here, the principles of typical SAR probe calibration methods are explained.

4.1 Probe calibration system that uses a calibration waveguide [8]–[10]

In SAR probe calibration, the waveguide method is widely used. A standard electric field is generated in a rectangular waveguide filled with phantom liquid, the probe is inserted in that, and the electric field and probe output voltage are compared. Figure 3 shows an outline of the calibration system.

The lower part of the waveguide is filled with air, and basic mode (TE_{10}) is propagated upwards from the coaxial waveguide converter of the lowest part. There is a dielectric slab between the liquid and propagating part of the waveguide. It is desirable that the depth of the phantom liquid be at least three times of the skin depth δ at the wavelength in the phantom liquid. The phantom liquid is a highly lossy media, and therefore the dielectric constants and thickness are adjusted so the dielectric slab becomes a quarter-wave plate in order to suppress reflection between the air and the phantom liquid. The calibration waveguide currently used is manufactured to have 10 to 20 dB or less reflection coefficient at the input port of the coaxial waveguide converter, while in a state filled with phantom liquid.

The dielectric slab can have a wide variety of structures and materials, however, NICT basically uses a slab made of a single layer of polyetheretherketone (PEEK) resin to obtain impedance matching with a thickness of around

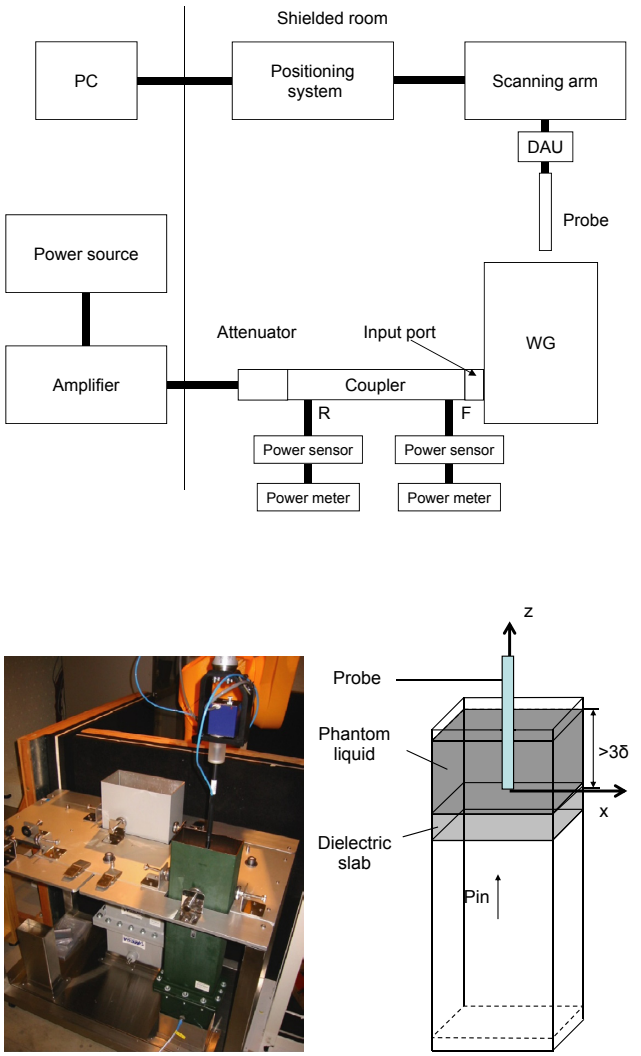

Fig. 3 SAR probe calibration system using a calibration waveguide, and schematic diagram

quarter wavelength. However, in order to actually obtain sufficient impedance matching, the effects of the phantom liquid dielectric constant, must be also considered and therefore prototyping and numerical simulation and so on must be performed to minutely adjust its thickness. Considering the environment of how it is used, the slab must also resist water and corrosion, and therefore both sides are coated with polyimide film. As scratches and bubbles on the film surface can cause inaccuracy of the calibration result. Considering the cutoff frequency, lower frequencies of calibration need larger waveguide size. Thus, considering handling of the measurement equipment, this method suits 700 MHz or higher frequencies.

In SAR calibration, the SAR probe measures the electric field in phantom liquid, and calibration is performed by correlating the output voltage of the probe with standard electric field. As long as the reflection of the liquid-filled part due to the dielectric slab is suppressed sufficiently, around the center of the calibration waveguide filled with phantom liquid, the distribution in the aperture surface is almost the same as the TE_{10} mode of the rectangular waveguide of the lower part. There is also attenuation due to the loss of the phantom liquid, therefore it has an exponential attenuation gradient in the direction of its depth (z direction in Fig. 3). The magnitude of the standard electric field to the depth direction z along the center axis can be obtained from input voltage P_{in} by the following equation.

$$E(z)=\sqrt{\frac{4\times P_{in}}{ab\delta\sigma}\times\exp\left(-\frac{2z}{\delta}\right)} \tag{6}$$

Here, a is the waveguide long side, b is the waveguide short side, δ is penetration depth of the phantom liquid, σ is conductivity of the phantom liquid, and z is distance from the surface of the dielectric slab. As the physical quantity SAR has no primary standard, traceability to the national standard is ensured by using a calibrated power meter to the measurement of input power P_{in}.

Also, near the center of the waveguide, electric field distribution of TE_{10} mode is dominant; thus, electric field distribution in the short side (y) direction is almost constant. Consequently, position z can be determined using $E(z)$ in Equation (6) and by approximating the distribution in the long side direction (x) using Equation (7) below.

$$\left|E(x)\right|^2 \cong E_{(z)}^2\left(\cos\left(\frac{\pi x}{a}\right)\right)^2 \tag{7}$$

4.2 Procedure for probe calibration using a calibration waveguide

The calibration procedure performed at NICT are shown below. The data was obtained using a commercially-available SAR measurement system (DASY52 manufactured by Schmidt & Partner Engineering AG).

① Dielectric constant measurement of phantom liquid

The dielectric constants (permittivity and conductivity) of the phantom liquid are measured. If the measured value deviates from the target value by ±3 % or more, then the dielectric constants of the phantom liquid must be adjusted.

② Measurement system preparation

As shown in Fig. 3, the calibration waveguide is installed near the scanning robot arm so the aperture surface is parallel to the floor. In this case, the

wave propagation direction in the waveguide is the z direction in Fig. 3. The calibration waveguide is filled with phantom liquid.

③ S_{11} Measurement of calibration waveguide

A network analyzer is used to measure S_{11} at the input port (see in Fig. 3) side of the calibration waveguide. This S_{11} value is used to determine the input power of the calibration waveguide when the calibration factor is calculated as described in ⑥ and ⑧.

④ Adjustment and determination of input power

First, connect a power meter directly to the waveguide-side port of the directional coupler, and adjust the output of the signal generator so the output power becomes the required level. Then, record the value (offset) of power meter at the port F (output of power in the forward direction from the directional coupler), then remove the power meter that is directly connected to the waveguide-port, and connect the waveguide directly to the directional coupler. During calibration, the output power is fine-tuned so the read value of power meter F connected to the directional coupler is the same as the offset value obtained above. Input power into the calibration waveguide P_{in} is 24.0 dBm (1 GHz or lower) or 22.0 dBm (1 GHz or higher) ± 0.1 dBm. The S_{11} of the waveguide is used to obtain the input power of the waveguide along with the read value of power meter F. The read value of the power meter of the R port is not directly used to control the input power, rather it is used to check whether excess power is not reflecting during calibration.

⑤ Instruction to the SAR measurement system of the position of the calibration waveguide

First, the SAR measurement system is launched, the SAR probe is normalized (vertical adjustment of the probe axis) by using the laser displacement meter in the DASY system. Next, instructions are given to the SAR measurement system using the reference point at the upper end of the calibration waveguide.

⑥ Preparation of calibration data sheet

For derivation of the calibration factor *Ki* by curve-fitting e (described in ⑧ below) to the measured values and theoretical values (Equation (6)), a dedicated data sheet is used for post-processing of data. First, in preparation, the following parameters are filled in the calibration data sheet.

- Dielectric constants of the Phantom liquid: Use measured value.
- S_{11} of calibration waveguide: Use measured value.
- Sensitivity ratio for each 3-axis sensor (free space): Input 1 as initial value.
- Boundary effect correction parameter: Use the value in the manufacturer's probe calibration certificate.

  It is also possible not to apply boundary effect correction, however, if correction is not used, then measured values may tend to be excessive near the surface [14].
- Diode compression parameter (DCP) correction factor: Use the value in the calibration certificate of the manufacturer. The DCP correction factor does not depend on conditions of the surroundings (air, phantom liquid); thus, calibration in free space (TEM cell or waveguide) is possible.

⑦ Running the calibration job

The calibration job sequence described below is run five times, and the measurement data (output voltage values for each sensor) is exported to the data sheet.

(a) Probe is moved to the specified position (detailed description in ⑧) of the waveguide center.
(b) The touch sensor connected to the probe is used to detect the dielectric slab surface (lowest surface of phantom liquid = z = 0 mm). Here, it must be considered that the actual measurement position is offset in the z direction from the probe tip of the sensor (1 mm on the EX3 DV4 probe).
(c) The RF output is turned on.
(d) Axial isotropy at z = 5 mm (measure at each 15 degree rotation angle) is measured.
(e) Z-direction (waveguide depth direction) scan (each 1 mm) of robot arm is executed.
Scan range of the z scan is changed according to the frequency (up to maximum 80 mm).
(f) After measurements are completed, system noise without RF input is measured.

⑧ Derivation of calibration factor

On the calibration data sheet, the optimization function such as in Excel Solver is used, and the measured data is numerically curve-fitted to match the theoretical formula for electric field distribution. For example, in the solver function in Excel, the Generalized Reduced Gradient method (GRG2) is used as an optimization algorithm. The curve-fitting steps are described below.

(a) Output data of three sensors is imported (z direction and axial isotropy data).

(b) Correction of diode characteristics (DCP).

(c) Data range used is set to fit curve (z direction).

Near the dielectric slab, change of sensitivity coefficients is not negligible due to the boundary effect caused by electrical coupling between the probe tip and dielectric slab [11]. On the other hand, at positions far from the dielectric slab, received field strength is declined due to loss of phantom liquid. Therefore, it is important to choose a fitting range where these effects are small.

NICT currently uses the curve fitting data ranges which determined empirically in Table 2, and SN ratios are evaluated at positions in the middle point of these curve fitting ranges. The setting of these curve fitting ranges is discontinuous between each frequency band, however, there are plans to optimize it in the future. The standard sizes of the waveguides are described in the Table.

(d) For the synthesized electric field of 3-axis sensor output obtained from Equation (2), the calibration factor K_i is optimized and the curve is numerically fitted so it fits toward the z direction attenuation curve of the theoretical electric field in Equation (6), and the calibration factor K_i is determined so the curve fitting relative errors are less than 0.01.

(e) The calibration factor K_i from the average of five measurements is determined.

4.3 Calibration system using temperature rise [8][9][15]

Temperature rise, electric field strength and SAR have a proportional relationship, as shown in Equation (1), if thermal diffusion due to thermal conduction and thermal emission and so forth is negligibly small. That is, if the specific heat and input power of the phantom liquid are known, calibration of an SAR probe can be performed using temperature rise.

A coaxial type calibration system is an example of a calibration system using this principle [8][15]. This device was developed by the National Physical Laboratory (NPL) aimed at application to probe calibration around 150 MHz or less. Figure 4 shows a diagram of the calibration device. Structure of this device is a coaxial waveguide of 50 Ω matching, and its end is shorted by a metal plate and a part of the center conductor is replaced by a liquid container. In the target frequency band, phantom liquid behaves like a conductor, and therefore a relatively uniform electric field distribution can be obtained near the center of the container filled with phantom liquid. Actually, it is feasible to

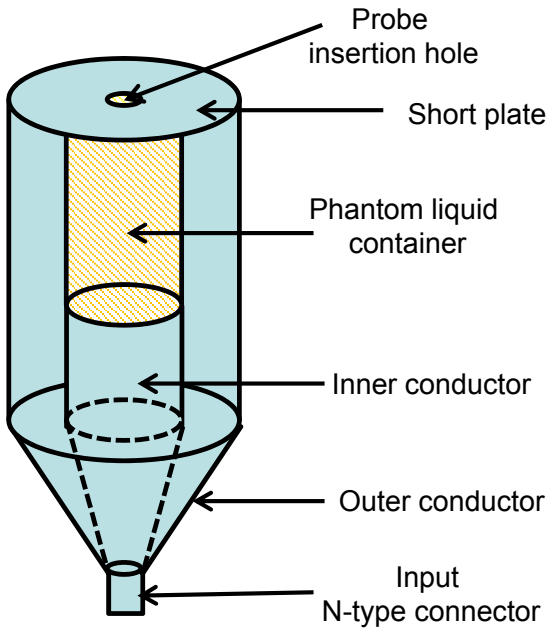

Fig. 4 Coaxial calibration system [8][15][16]

Table 2 Ranges of curve fitting data for waveguide calibration

Frequency (MHz)	733	835	900	1450	1624	1767.5	1950	2018	2450	2585	3500	5200
Waveguide standard(EIAJ)	WRI-9			WRI-14			WRI-22				WRI-40	WRI-48
Curve fitting range z (mm)	20-40	10-30	10-30	10-30	10-30	6-37	6-30	6-37	6-37	8-15	4-7	8-12

apply frequencies from several MHz to up to about 450 MHz.

4.4 Calibration system in phantom liquid using a standard antenna [13]

A calibration method that does not use a calibration waveguide have been developed—the standard electric field method using a standard antenna with known structure and radiation characteristics was used with a container filled with phantom liquid. Figures 5 and 6 are diagrams of calibration systems. First, gain of the standard antenna is obtained as follows. The steps are, first, an identical pair of antennas are installed in a container filled with phantom liquid, the distance between the antennas is changed, then S_{21} is obtained at each distance, and gain of the standard antenna installed on the tank bottom surface is obtained (Fig. 5). Next, the probe to be calibrated is attached to an opposing robot arm, its output is measured, and antenna calibration is performed (Fig. 6).

When determining the gain of a standard antenna, use the reflection loss and characteristics of distance attenuation between antennas, and use the two-antenna method with the Friis' transmission formula extended to lossy media. In phantom liquid, its sharp attenuation differs from in free space; thus, it is difficult to perform calibration in the far field region like in usual antenna calibrations. Therefore, considering attenuation in phantom liquid and effects in very near field, the Friis' transmission formula was extended until the Fresnel domain. As the standard antenna in phantom liquid, a dipole antenna that has a simple structure with simple theoretical analysis and detached waveguide antenna were proposed.

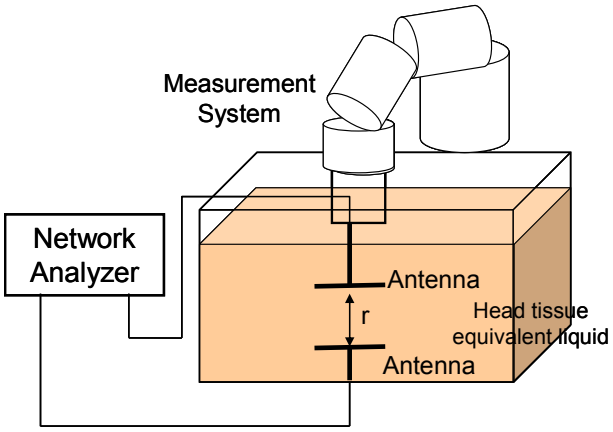

Fig. 5 Absolute gain calibration of standard antenna in phantom liquid

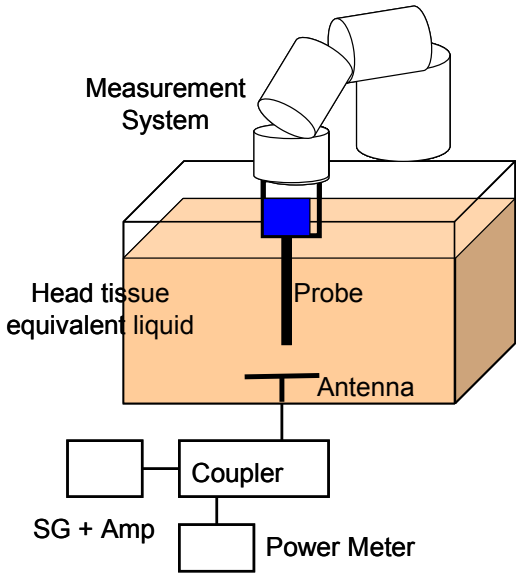

Fig. 6 Probe calibration using standard antenna in phantom liquid

Table 3 Uncertainty of liquid dielectric constant measurement

	a		b	C	$u_i = (a/b) \times (c)$	
Source of uncertainty	Uncertainty value (±%)	Probability distribution	Divisor	Sensitivity coefficient c_i	Standard uncertainty (±%)	Degrees of freedom v_i or v_{eff}
Repeatability of measurements		Normal	1	1		N-1
Deviation from standard value of dielectric constant (ε_r' or σ)		Uniform	$\sqrt{3}$	1		N-1
Uncertainty of network analyzer and other		Uniform	$\sqrt{3}$	1		∞
Combined expanded uncertainty						

5 Example of SAR probe calibration uncertainty evaluation by calibration waveguide method

Described here is an example of an actual SAR probe calibration result and evaluation of uncertainty of a method using a calibration waveguide. The dielectric constants of phantom liquid and several other items are frequency dependent; thus, evaluation of each frequency is required. This evaluation method of dielectric constant complies with IEC 62209–1.

5.1 Uncertainty sources and method to evaluate each item

(1) Input Power

The value of uncertainty in the calibration certificate of the terminal power measurement power sensor was used. A normal probability distribution was assumed.

(2) Misalignment of Calibration Waveguide

The tolerance value for misalignment of the calibration waveguide input end can be derived from Equation (8) below. Therefore, in this study, measurements were made for the output terminal reflection coefficient of the terminal type power sensor, device input end and directional coupler, and evaluations were made on misalignment. A U-shaped probability distribution was assumed.

$$M = 1 - \frac{(1-|\Gamma_p|^2)\times(1-|\Gamma_s||\Gamma_c|)^2}{(1+|\Gamma_s||\Gamma_p|)^2} \quad (8)$$

Here, M is the maximum mismatch tolerance value, Γ_S is the reflection coefficient at the output end of directional coupler, and Γ_P is the reflection coefficient of the terminal power sensor.

(3) Data Acquisition Unit (DAU)

Here, the value of uncertainty in the calibration certificate of the manufacturer was used. A normal probability distribution was assumed.

(4) Permittivity and Conductivity of Phantom Liquid

For uncertainty evaluation of dielectric measurements of the phantom liquid, a possible way is to use the typical accuracy provided by the manufacturer of the permittivity measurement probe [17]–[20]. This paper is based on the evaluation method of IEC62209–1 [8].

① Repeatability of Measurements

At each frequency, permittivity and conductivity of the phantom liquid is measured 10 times and the standard deviation obtained is divided by the average value measured to obtain the tolerance value. A normal probability distribution is used.

② Deviation from Standard Value of Dielectric Constants

The deviation of the average measured values form the target values is considered as the tolerance.

A rectangular probability distribution is used.

③ Uncertainty of Network Antennas and Other

This time, to derive uncertainty of the network analyzer, uncertainty evaluation software was employed that uses the Monte Carlo method and was manufactured by NPL in the UK. A rectangular probability distribution is used.

Table 3 shows the uncertainty budget of IEC62209–1 [8].

(5) Deviation from Target Values of Permittivity and Conductivity of Phantom Liquid during Calibration

At each frequency, the deviation of the dielectric constant of the phantom liquid used from the target value is evaluated. An adjustment is made so the dielectric constant of the phantom liquid is within ± 3% of the target value at all frequencies in NICT, and therefore 3 % is used here. A uniform probability distribution was assumed.

(6) Uniformity of Electric Field Distribution

For the electric field distribution, electric field distribution near the center of the calibration waveguide is measured, and evaluation is conducted on the maximum deviation from the approximation formula of TE_{10} mode, by squared and cosign square functions of the electric field strength measured. Here, for electric field distribution, the approximation Equation (7) shown earlier was used. For measurement of the electric field distribution, evaluation was conducted at a measurement position (z direction) with distance between the probe tip and dielectric slab at 10 mm (835 to 2,450 MHz) or 5 mm (5 GHz band), and measurement range of ±20 mm from the center in the waveguide length direction. A uniform probability distribution was assumed.

(7) Probe Position

Probe position determination uncertainty caused by inaccurate position detection in the z direction of the robot was evaluated by using distance error (Δz) during surface detection, and penetration depth δ, in Equation (9).

$$\Delta SAR = (1 - e^{\frac{-2\Delta z}{\delta}}) \quad (9)$$

Δz: Distance between the probe tip and dielectric slab surface, during surface detection (z = 0)

Here, Δz is the z = 0 position detection error of the robot in phantom liquid, that is, equivalent to the detection error of the dielectric slab surface position. Here, the SAR measurement system used at NICT employs a spring mechanism in the probe connector of the output data acquisition unit (DAU), meaning this also includes error caused by play in the probe mounted to the DAU. For the evaluation method, a flat plate was hung vertically above the phantom liquid, surface detection was performed on that liquid, and a feeler gauge was used to measure the distance between the surface and probe tip. A uniform probability distribution was assumed.

(8) Linearity of SAR Probe

The 0.6 % linearity uncertainty in the calibration certificate of the manufacturer was used. A normal probability distribution was assumed.

(9) Data S/N Ratio

The output voltage of the DAU with/without RF signal input was used to obtain the S/N ratio. A normal probability distribution was assumed.

(10) Variability of Calibration Factor

Calibration was conducted five times, and relative standard deviation of these data was used. A normal probability distribution was assumed.

First, Tables 4 to 15 below show examples for relative uncertainty evaluation. For uncertainty values cited from the calibration certificate, for example, a normal distribution was assumed and 2 was assumed as the divisor.

Table 4 Example of evaluating waveguide calibration uncertainty (733 MHz, EX3DV4 Probe)

Source of tolerance	Tolerance a [%]	Probability distribution	Divisor b	Sensitivity coefficient c_i	Standard uncertainty (±%) u=(a / b)×c_i	Degrees of freedom v_i or v_{eff}
Input power(k=2)	3.30	Normal	2	1	1.65	∞
Waveguide mismatch	2.53	U	$\sqrt{2}$	1	1.79	∞
DAU uncertainty(k=2)	1.50	Normal	2	1	0.75	∞
Measurement of phantom liquid dielectric constant (conductivity)	1.10	Normal	1	1	1.10	9
Measurement of phantom liquid dielectric constant (permittivity)	1.03	Normal	1	1	1.03	9
Deviation from standard value of phantom liquid (conductivity)	3.00	Uniform	$\sqrt{3}$	1	1.73	∞
Deviation from standard value of phantom liquid (permittivity)	3.00	Uniform	$\sqrt{3}$	1	1.73	∞
Electric field uniformity	0.13	Uniform	$\sqrt{3}$	1	0.08	
Probe positioning	0.30	Uniform	$\sqrt{3}$	1	0.17	
Probe linearity (k=2)	0.60	Normal	2	1	0.30	∞
Output voltage S/N ratio	0.63	Normal	1	1	0.63	∞
Measurement data variability (measure five times)	0.32	Normal	$\sqrt{N}$(N=5)	1	0.14	4
Combined standard uncertainty					3.91	
Coverage factor k (95% confidence level)					1.96	812
Expanded uncertainty					7.68	

Table 5 Example of waveguide calibration uncertainty (835 MHz, EX3DV4 Probe)

Source of tolerance	Tolerance a [%]	Probability distribution	Divisor b	Sensitivity coefficient c_i	Standard uncertainty (±%) u=(a / b)×c_i	Degrees of freedom v_i or v_{eff}
Input power(k=2)	3.30	Normal	2	1	1.65	∞
Waveguide mismatch	3.10	U	$\sqrt{2}$	1	2.19	∞
DAU uncertainty(k=2)	1.50	Normal	2	1	0.75	∞
Measurement of phantom liquid dielectric constant (conductivity)	0.86	Normal	1	1	0.86	9
Measurement of phantom liquid dielectric constant (permittivity)	1.28	Normal	1	1	1.28	9
Deviation from standard value of phantom liquid (conductivity)	0.40	Uniform	$\sqrt{3}$	1	1.73	∞
Deviation from standard value of phantom liquid (permittivity)	3.00	Uniform	$\sqrt{3}$	1	1.73	∞
Electric field uniformity	0.40	Uniform	$\sqrt{3}$	1	0.23	∞
Probe positioning	0.31	Uniform	$\sqrt{3}$	1	0.18	∞
Probe linearity (k=2)	0.60	Normal	2	1	0.30	∞
Output voltage S/N ratio	0.63	Normal	1	1	0.63	∞
Measurement data variability (measure five times)	0.41	Normal	$\sqrt{N}$(N=5)	1	0.18	4
Combined standard uncertainty					4.13	
Coverage factor k (95% confidence level)					1.96	818
Expanded uncertainty					8.11	

Table 6 Example of waveguide calibration uncertainty (900 MHz, EX3DV4 Probe)

Source of tolerance	Tolerance a [%]	Probability distribution	Divisor b	Sensitivity coefficient c_i	Standard uncertainty (±%) u=(a / b)×c_i	Degrees of freedom v_i or v_{eff}
Input power	3.30	Normal	2	1	1.65	∞
Waveguide mismatch	1.24	U	$\sqrt{2}$	1	0.88	∞
DAU uncertainty	1.50	Normal	2	1	0.75	∞
Measurement of phantom liquid dielectric constant (conductivity)	1.32	Normal	1	1	1.32	9
Measurement of phantom liquid dielectric constant (permittivity)	1.28	Normal	1	1	1.28	9
Deviation from standard value of phantom liquid (conductivity)	0.42	Uniform	$\sqrt{3}$	1	1.73	∞
Deviation from standard value of phantom liquid (permittivity)	3.00	Uniform	$\sqrt{3}$	1	1.73	∞
Electric field uniformity	0.42	Uniform	$\sqrt{3}$	1	0.24	∞
Probe positioning	0.33	Uniform	$\sqrt{3}$	1	0.19	∞
Probe linearity	0.60	Normal	2	1	0.30	∞
Output voltage S/N ratio	0.70	Normal	1	1	0.70	∞
Measurement data variability (measure five times)	0.57	Normal	$\sqrt{N}$(N=5)	1	0.25	4
Combined standard uncertainty					3.77	
Coverage factor k (95% confidence level)					1.97	313
Expanded uncertainty					7.41	

Table 7 Example of waveguide calibration uncertainty (1,450 MHz, EX3DV4 Probe)

Source of tolerance	Tolerance a [%]	Probability distribution	Divisor b	Sensitivity coefficient c_i	Standard uncertainty (±%) u=(a / b)×c_i	Degrees of freedom v_i or v_{eff}
Input power(k=2)	3.30	Normal	2	1	1.65	∞
Waveguide mismatch	1.03	U	$\sqrt{2}$	1	0.73	∞
DAU uncertainty(k=2)	1.50	Normal	2	1	0.75	∞
Measurement of phantom liquid dielectric constant (conductivity)	0.82	Normal	1	1	0.82	9
Measurement of phantom liquid dielectric constant (permittivity)	1.53	Normal	1	1	1.53	9
Deviation from standard value of phantom liquid (conductivity)	0.11	Uniform	$\sqrt{3}$	1	1.73	∞
Deviation from standard value of phantom liquid (permittivity)	3.00	Uniform	$\sqrt{3}$	1	1.73	∞
Electric field uniformity	0.11	Uniform	$\sqrt{3}$	1	0.06	∞
Probe positioning	0.42	Uniform	$\sqrt{3}$	1	0.24	∞
Probe linearity (k=2)	0.60	Normal	2	1	0.30	∞
Output voltage S/N ratio	0.76	Normal	1	1	0.76	∞
Measurement data variability (measure five times)	0.30	Normal	$\sqrt{N}$(N=5)	1	0.13	4
Combined standard uncertainty					3.69	
Coverage factor k (95% confidence level)					1.97	278
Expanded uncertainty					7.26	

Table 8 Example of waveguide calibration uncertainty (1,624 MHz, EX3DV4 Probe)

Source of tolerance	Tolerance a [%]	Probability distribution	Divisor b	Sensitivity coefficient c_i	Standard uncertainty (±%) u=(a / b)×c_i	Degrees of freedom v_i or v_{eff}
Input power(k=2)	3.30	Normal	2	1	1.65	∞
Waveguide mismatch	3.94	U	$\sqrt{2}$	1	2.79	∞
DAU uncertainty(k=2)	1.50	Normal	2	1	0.75	∞
Measurement of phantom liquid dielectric constant (conductivity)	0.77	Normal	1	1	0.77	9
Measurement of phantom liquid dielectric constant (permittivity)	1.64	Normal	1	1	1.64	9
Deviation from standard value of phantom liquid (conductivity)	0.34	Uniform	$\sqrt{3}$	1	1.73	∞
Deviation from standard value of phantom liquid (permittivity)	3.00	Uniform	$\sqrt{3}$	1	1.73	∞
Electric field uniformity	0.34	Uniform	$\sqrt{3}$	1	0.20	∞
Probe positioning	0.46	Uniform	$\sqrt{3}$	1	0.26	∞
Probe linearity (k=2)	0.60	Normal	2	1	0.30	∞
Output voltage S/N ratio	0.95	Normal	1	1	0.95	∞
Measurement data variability (measure five times)	0.77	Normal	$\sqrt{N}$(N=5)	1	0.34	4
Combined standard uncertainty					4.64	
Coverage factor k (95% confidence level)					1.96	544
Expanded uncertainty					9.12	

Table 9 Example of waveguide calibration uncertainty (1,767.5 MHz, EX3DV4 Probe)

Source of tolerance	Tolerance a [%]	Probability distribution	Divisor b	Sensitivity coefficient c_i	Standard uncertainty (±%) u=(a / b)×c_i	Degrees of freedom v_i or v_{eff}
Input power(k=2)	3.30	Normal	2	1	1.65	∞
Waveguide mismatch	2.77	U	$\sqrt{2}$	1	1.96	∞
DAU uncertainty(k=2)	1.50	Normal	2	1	0.75	∞
Measurement of phantom liquid dielectric constant (conductivity)	0.72	Normal	1	1	0.72	9
Measurement of phantom liquid dielectric constant (permittivity)	1.70	Normal	1	1	1.70	9
Deviation from standard value of phantom liquid (conductivity)	0.25	Uniform	$\sqrt{3}$	1	1.73	∞
Deviation from standard value of phantom liquid (permittivity)	3.00	Uniform	$\sqrt{3}$	1	1.73	∞
Electric field uniformity	0.25	Uniform	$\sqrt{3}$	1	0.15	∞
Probe positioning	0.48	Uniform	$\sqrt{3}$	1	0.28	∞
Probe linearity (k=2)	0.60	Normal	2	1	0.30	∞
Output voltage S/N ratio	0.47	Normal	1	1	0.47	∞
Measurement data variability (measure five times)	0.33	Normal	$\sqrt{N}$(N=5)	1	0.15	4
Combined standard uncertainty					4.12	
Coverage factor k (95% confidence level)					1.97	299
Expanded uncertainty					8.11	

Table 10 Example of waveguide calibration uncertainty (1,950 MHz, EX3DV4 Probe)

Source of tolerance	Tolerance a [%]	Probability distribution	Divisor b	Sensitivity coefficient c_i	Standard uncertainty (±%) u=(a / b)×c_i	Degrees of freedom v_i or v_{eff}
Input power(k=2)	3.30	Normal	2	1	1.65	∞
Waveguide mismatch	0.48	U	$\sqrt{2}$	1	0.34	∞
DAU uncertainty(k=2)	1.50	Normal	2	1	0.75	∞
Measurement of phantom liquid dielectric constant (conductivity)	0.95	Normal	1	1	0.95	9
Measurement of phantom liquid dielectric constant (permittivity)	1.99	Normal	1	1	1.99	9
Deviation from standard value of phantom liquid (conductivity)	0.99	Uniform	$\sqrt{3}$	1	1.73	∞
Deviation from standard value of phantom liquid (permittivity)	3.00	Uniform	$\sqrt{3}$	1	1.73	∞
Electric field uniformity	0.99	Uniform	$\sqrt{3}$	1	0.57	∞
Probe positioning	0.49	Uniform	$\sqrt{3}$	1	0.28	∞
Probe linearity (k=2)	0.60	Normal	2	1	0.30	∞
Output voltage S/N ratio	0.52	Normal	1	1	0.52	∞
Measurement data variability (measure five times)	0.28	Normal	$\sqrt{N}$(N=5)	1	0.13	4
Combined standard uncertainty					3.88	
Coverage factor k (95% confidence level)					1.98	123
Expanded uncertainty					7.68	

Table 11 Example of waveguide calibration uncertainty (2,018 MHz, EX3DV4 Probe)

Source of tolerance	Tolerance a [%]	Probability distribution	Divisor b	Sensitivity coefficient c_i	Standard uncertainty (±%) u=(a / b)×c_i	Degrees of freedom v_i or v_{eff}
Input power(k=2)	3.30	Normal	2	1	1.65	∞
Waveguide mismatch	0.50	U	$\sqrt{2}$	1	0.35	∞
DAU uncertainty(k=2)	1.50	Normal	2	1	0.75	∞
Measurement of phantom liquid dielectric constant (conductivity)	1.42	Normal	1	1	1.42	9
Measurement of phantom liquid dielectric constant (permittivity)	2.12	Normal	1	1	2.12	9
Deviation from standard value of phantom liquid (conductivity)	0.31	Uniform	$\sqrt{3}$	1	1.73	∞
Deviation from standard value of phantom liquid (permittivity)	3.00	Uniform	$\sqrt{3}$	1	1.73	∞
Electric field uniformity	0.31	Uniform	$\sqrt{3}$	1	0.18	∞
Probe positioning	0.50	Uniform	$\sqrt{3}$	1	0.29	∞
Probe linearity (k=2)	0.60	Normal	2	1	0.30	∞
Output voltage S/N ratio	0.52	Normal	1	1	0.52	∞
Measurement data variability (measure five times)	0.55	Normal	$\sqrt{N}$(N=5)	1	0.25	4
Combined standard uncertainty					4.06	
Coverage factor k (95% confidence level)					1.98	101
Expanded uncertainty					8.05	

Table 12 Example of waveguide calibration uncertainty (2,450 MHz, EX3DV4 Probe)

Source of tolerance	Tolerance a [%]	Probability distribution	Divisor b	Sensitivity coefficient c_i	Standard uncertainty (±%) u=(a / b)×c_i	Degrees of freedom v_i or v_{eff}
Input power(k=2)	3.30	Normal	2	1	1.65	∞
Waveguide mismatch	0.84	U	$\sqrt{2}$	1	0.59	∞
DAU uncertainty(k=2)	1.50	Normal	2	1	0.75	∞
Measurement of phantom liquid dielectric constant (conductivity)	1.10	Normal	1	1	1.10	9
Measurement of phantom liquid dielectric constant (permittivity)	2.14	Normal	1	1	2.14	9
Deviation from standard value of phantom liquid (conductivity)	0.80	Uniform	$\sqrt{3}$	1	1.73	∞
Deviation from standard value of phantom liquid (permittivity)	3.00	Uniform	$\sqrt{3}$	1	1.73	∞
Electric field uniformity	0.80	Uniform	$\sqrt{3}$	1	0.46	∞
Probe positioning	0.64	Uniform	$\sqrt{3}$	1	0.37	∞
Probe linearity (k=2)	0.60	Normal	2	1	0.30	∞
Output voltage S/N ratio	0.93	Normal	1	1	0.93	∞
Measurement data variability (measure five times)	0.57	Normal	$\sqrt{N}$(N=5)	1	0.25	4
Combined standard uncertainty					4.10	
Coverage factor k (95% confidence level)					1.98	114
Expanded uncertainty					8.12	

Table 13 Example of waveguide calibration uncertainty (2,585 MHz, EX3DV4 Probe)

Source of tolerance	Tolerance a [%]	Probability distribution	Divisor b	Sensitivity coefficient c_i	Standard uncertainty (±%) $u=(a / b)\times c_i$	Degrees of freedom v_i or v_{eff}
Input power(k=2)	3.30	Normal	2	1	1.65	∞
Waveguide mismatch	5.34	U	$\sqrt{2}$	1	3.78	∞
DAU uncertainty(k=2)	1.50	Normal	2	1	0.75	∞
Measurement of liquid dielectric constant (conductivity)	1.11	Normal	1	1	1.11	9
Measurement of liquid dielectric constant (permittivity)	3.42	Normal	1	1	3.42	9
Deviation from standard value of liquid (conductivity)	0.94	Uniform	$\sqrt{3}$	1	1.73	∞
Deviation from standard value of liquid (permittivity)	3.00	Uniform	$\sqrt{3}$	1	1.73	∞
Electric field uniformity	0.94	Uniform	$\sqrt{3}$	1	0.54	∞
Probe positioning	0.69	Uniform	$\sqrt{3}$	1	0.40	∞
Probe linearity (k=2)	0.60	Normal	2	1	0.30	∞
Output voltage S/N ratio	0.65	Normal	1	1	0.65	∞
Measurement data variability (measure five times)	0.34	Normal	$\sqrt{N}$(N=5)	1	0.15	4
Combined standard uncertainty					6.12	
Coverage factor k (95% confidence level)					1.99	91
Expanded uncertainty					12.2	

Table 14 Example of waveguide calibration uncertainty (3,500 MHz, EX3DV4 Probe)

Source of tolerance	Tolerance a [%]	Probability distribution	Divisor b	Sensitivity coefficient c_i	Standard uncertainty (±%) $u=(a / b)\times c_i$	Degrees of freedom v_i or v_{eff}
Input power(k=2)	3.30	Normal	2	1	1.65	∞
Waveguide mismatch	3.17	U	$\sqrt{2}$	1	2.24	∞
DAU uncertainty(k=2)	1.50	Normal	2	1	0.75	∞
Measurement of liquid dielectric constant (conductivity)	1.22	Normal	1	1	1.22	9
Measurement of liquid dielectric constant (permittivity)	2.29	Normal	1	1	2.29	9
Deviation from standard value of liquid (conductivity)	3.87	Uniform	$\sqrt{3}$	1	1.73	∞
Deviation from standard value of liquid (permittivity)	3.00	Uniform	$\sqrt{3}$	1	1.73	∞
Electric field uniformity	3.87	Uniform	$\sqrt{3}$	1	2.23	∞
Probe positioning	0.87	Uniform	$\sqrt{3}$	1	0.50	∞
Probe linearity (k=2)	0.60	Normal	2	1	0.30	∞
Output voltage S/N ratio	0.08	Normal	1	1	0.08	∞
Measurement data variability (measure five times)	1.27	Normal	$\sqrt{N}$(N=5)	1	0.57	4
Combined standard uncertainty					5.17	
Coverage factor k (95% confidence level)					1.97	214
Expanded uncertainty					10.2	

Table 15 Example of waveguide calibration uncertainty (5,200 MHz, EX3DV4 Probe)

Source of tolerance	Tolerance a [%]	Probability distribution	Divisor b	Sensitivity coefficient c_i	Standard uncertainty (±%) u=(a / b)×c_i	Degrees of freedom v_i or v_{eff}
Input power(k=2)	3.30	Normal	2	1	1.65	∞
Waveguide mismatch	1.57	U	$\sqrt{2}$	1	1.11	∞
DAU uncertainty(k=2)	1.50	Normal	2	1	0.75	∞
Measurement of liquid dielectric constant (conductivity)	1.09	Normal	1	1	1.09	9
Measurement of liquid dielectric constant (permittivity)	2.60	Normal	1	1	2.60	9
Deviation from standard value of liquid (conductivity)	1.94	Uniform	$\sqrt{3}$	1	1.73	∞
Deviation from standard value of liquid (permittivity)	3.00	Uniform	$\sqrt{3}$	1	1.73	∞
Electric field uniformity	1.94	Uniform	$\sqrt{3}$	1	1.12	∞
Probe positioning	1.43	Uniform	$\sqrt{3}$	1	0.83	∞
Probe linearity (k=2)	0.60	Normal	2	1	0.30	∞
Output voltage S/N ratio	0.37	Normal	1	1	0.37	∞
Measurement data variability (measure five times)	0.52	Normal	$\sqrt{N}$(N=5)	1	0.23	4
Combined standard uncertainty					4.55	
Coverage factor k (95% confidence level)					1.99	82
Expanded uncertainty					9.05	

Table 16 Uncertainty sources and standard uncertainty in waveguide calibration

Frequency (MHz)	733	835	900	1450	1624	1767.5	1950	2018	2450	2585	3500	5200
Waveguide mismatch(%)	1.79	2.19	0.88	0.73	2.79	1.96	0.34	0.35	0.59	3.78	2.24	1.11
Dielectric constant measurement (conductivity) (%)	1.10	0.86	1.32	0.82	0.77	0.72	0.95	1.42	1.10	1.11	1.22	1.09
Dielectric constant measurement (permittivity) (%)	1.03	1.28	1.28	1.53	1.64	1.70	1.99	2.12	2.14	3.42	2.29	2.60
Expanded uncertainty(%)	7.68	8.11	7.41	7.26	9.12	8.11	7.68	8.05	8.12	12.2	10.2	9.05

Table 17 Example of calibration result (EX3DV4)

Frequency (MHz)	733	835	900	1950	2450	3500	5200
Calibration factor K [μV/(V/m)^2]	3.90	3.55	3.50	3.03	2.73	2.92	2.16
Previous calibration result	3.89	3.59	3.49	3.11	2.81	2.98	2.00
Deviation (%)	0.23	–1.14	0.49	–2.39	–2.74	–1.88	8.15
Ratio of deviation and expanded uncertainty	0.03	–0.14	0.04	–0.33	–0.35	–0.19	0.89

Table 16 shows a list of typical uncertainty sources, uncertainties, and expanded uncertainties, from the results described above. In this evaluation, expanded uncertainties overall tended to increase along with higher frequencies. Looking at individual sources, waveguide mismatch is not frequency dependent because of adjustments to match each frequency, however, there is a need to consider it at each frequency. On the other hand, uncertainty of permittivity and conductivity increases along with higher frequencies; thus, there is a need for very accurate measurements at high frequencies.

As an example of calibration results, Table 17 shows how results of SAR probe EX3DV4 calibration performed at NICT differ from the results of last year.

The ratios of differences from the calibration results data of last time and expanded uncertainty were also presented for reference.

6 Conclusion

This paper described the calibration method, principles, calibration results and an uncertainty evaluation example for the SAR probe. A primary standard has not been established for SAR probe calibration yet, and therefore it is desirable to be able to apply calibration that uses multiple principles. In addition, in order to ensure reliability, it is also important to have mutual comparisons between multiple calibration institutions. It was confirmed that calibration results of NICT are within the range of calibration uncertainty (approximately 10 %) of the NPL of the UK and the probe manufacturer (ISO17025 certified calibration institution) [21]. In the future more detailed evaluation of uncertainty is necessary, including an optimization of the curve-fitting range in calibration and other sources such as boundary effect. There are also plans to extend the calibration service frequencies. Furthermore, uncertainty evaluation of the methods that use devices other than calibration waveguide will be provided.

Acknowledgments

Part of this research was implemented under Ministry of Internal Affairs and Communications contracted research (Electromagnetic waves safety evaluation technology).

References

1 Ministry of Posts and Telecommunications, Telecommunications Technology Council, Report of Inquiry No.38(1990)(In Japanese)
2 Ministry of Posts and Telecommunications, Telecommunications Technology Council, Report of Inquiry, No.89(1997)(In Japanese)
3 ICNIRP Guidelines for limiting exposure to time-varying electric magnetic, and electromagnetic fields (up to 300 GHz), Health Physics, 77(4), pp.494-522(1998)
4 Evaluating Compliance with FCC Guidelines for Human Exposure to Radiofrequency Electromagnetic Fields, FCC OET Bulletin 65 OET Supplement C, (1997)
5 IEEE C95.1-2005 - IEEE Standard for Safety Levels with Respect to Human Exposure to Radio Frequency Electromagnetic Fields, 3 kHz to 300 GHz, (2005)
6 ICNIRP Guidelines for limiting exposure for limiting exposure to time-varying electric and magnetic fields (1Hz – 100 kHz), Health Physics, 99(6), pp.818-836(2010)
7 Ministry of Internal Affairs and Communications, Information and Communications Council, Partial Report of Inquiry No 118(2011)(In Japanese).
8 IEC 62209-1:2016, Human exposure to radio frequency fields from hand-held and body-mounted wireless communication devices - Human models, instrumentation, and procedures - Part 1: Procedure to determine the specific absorption rate (SAR) for hand-held devices used in close proximity to the ear (frequency range of 300 MHz to 3 GHz), (2016).
9 IEC 62209-2:2010 : Human exposure to radio frequency fields from hand-held and body-mounted wireless communication devices - Human models, instrumentation, and procedures - Part 2: Procedure to determine the specific absorption rate (SAR) for wireless communication devices used in close proximity to the human body (frequency range of 30 MHz to 6 GHz), 2010
10 IEEE Standard 1528-2013 - IEEE Recommended Practice for Determining the Peak Spatial-Average Specific Absorption Rate (SAR) in the Human Head from Wireless Communications Devices: Measurement Techniques, 2013
11 Katja Pokovic, "Advanced Electromagnetic Probes for Near-Field Evaluations",, Swiss Federal Institute of Technology, Zurich Doctoral Dissertation ETH No. 13334, 1999.
12 Katja Pokovic, Thomas Schmid, and Niels Kuster, Millimeter-Resolution E-Field Probe for Isotropic Measurement in Lossy Media Between 100 MHz and 20 GHz, IEEE TRANSACTIONS ON INSTRUMENTATION AND MEASUREMENTS, vol.49, no.4, AUGUST 2000
13 Hamada et.al., Expansion of the SAR-probe calibration system using the reference dipole antenna in head-simulating liquid", Tech Rep. IEICE, EMCJ 109(370), 135-140, 2010 (Jan. 2010).(In Japanese)
14 Iwatani et.al: A Study on Influence of Boundary Effect in Specific Absorption Rate Measurement of Radio Communication Equipment, 2015 Annual Conference of IEICE, B-4-24, 2015 (In Japanese)
15 Low-frequency (10-450 MHz) Coaxial SAR Calibration System http://www.npl.co.uk/instruments/products/rf-microwave/low-frequency-coaxial-sar-calibration-system/
16 Loader, B.G, Gregory A.P. Bownds, D., Coaxial artefact standard for specific absorption rate 100 kHz to 400 MHz, Progress in Electromagnetic Research Symposium (PIERS), 23-27 March, 2009, Beijing, China
17 Aikyo et.al, "Probe calibration system for SAR measurement and evaluation of calibration uncertainty 2 - 1450MHz/1950MHz system and depth effect of tissue equivalent liquid on calibration –," Tech Rep. IEICE, EMCJ2005-112, pp.33-38, Nov. 2005.(In Japanese)
18 Aikyo et.al "Probe calibration system for SAR measurement and evaluation of calibration uncertainty : 900MHz band system in compliance with ARIB standard," Tech Rep. IEICE, EMCJ2004-126, pp.55-59, Jan. 2005.(In Japanese)
19 Ichino et.al., "Uncertainty of SAR measurement of cellular phones, " Tech Rep. IEICE, EMCJ2004-125, pp.49-54, Jan. 2005.(In Japanese)
20 Hamada et.al., Uncertainty of Specific Absorption Rate Probe Calibration Using Waveguide Systems, Tech Rep. IEICE, EMCJ 111(492), 19-23, 2012 (In Japanese)
21 Loader et.al., SAR probe calibration: the results of an intercomparison study, EMC Kyoto 2009, pp. 81-83, 2009

Lira HAMADA, Dr. Eng.
Senior Researcher, Electromagnetic Compatibility Laboratory, Applied Electromagnetic Research Institute
Bioelectromagnetics

Soichi WATANABE, Dr. Eng.
Research manager, Electromagnetic Compatibility Laboratory, Applied Electromagnetic Research Institute
Bioelectromagnetics